The contribution of hydrophobic residues in the pore-forming region of the ryanodine receptor channel to block by large tetraalkylammonium cations and *Shaker* B inactivation peptides

Sammy A. Mason,[1] Cedric Viero,[1] Joanne Euden,[1] Mark Bannister,[1] Duncan West,[1] S.R. Wayne Chen,[2] and Alan J. Williams[1]

[1]Institute of Molecular and Experimental Medicine, Wales Heart Research Institute, School of Medicine, Cardiff University, Cardiff CF14 4XN, Wales, UK

[2]Department of Physiology and Pharmacology, University of Calgary, Calgary, Alberta T2N 4N1, Canada

Although no high-resolution structural information is available for the ryanodine receptor (RyR) channel pore-forming region (PFR), molecular modeling has revealed broad structural similarities between this region and the equivalent region of K^+ channels. This study predicts that, as is the case in K^+ channels, RyR has a cytosolic vestibule lined with predominantly hydrophobic residues of transmembrane helices (TM10). In K^+ channels, this vestibule is the binding site for blocking tetraalkylammonium (TAA) cations and *Shaker* B inactivation peptides (*Sh*BPs), which are stabilized by hydrophobic interactions involving specific residues of the lining helices. We have tested the hypothesis that the cytosolic vestibule of RyR fulfils a similar role and that TAAs and *Sh*BPs are stabilized by hydrophobic interactions with residues of TM10. Both TAAs and *Sh*BPs block RyR from the cytosolic side of the channel. By varying the composition of TAAs and *Sh*BPs, we demonstrate that the affinity of both species is determined by their hydrophobicity, with variations reflecting alterations in the dissociation rate of the bound blockers. We investigated the role of TM10 residues of RyR by monitoring block by TAAs and *Sh*BPs in channels in which the hydrophobicity of individual TM10 residues was lowered by alanine substitution. Although substitutions changed the kinetics of TAA interaction, they produced no significant changes in *Sh*BP kinetics, indicating the absence of specific hydrophobic sites of interactions between RyR and these peptides. Our investigations (a) provide significant new information on both the mechanisms and structural components of the RyR PFR involved in block by TAAs and *Sh*BPs, (b) highlight important differences in the mechanisms and structures determining TAA and *Sh*BP block in RyR and K^+ channels, and (c) demonstrate that although the PFRs of these channels contain analogous structural components, significant differences in structure determine the distinct ion-handling properties of the two species of channel.

The Journal of General Physiology

INTRODUCTION

The cardiac isoform of the ryanodine receptor (RyR2) is an ion channel that provides the pathway for release of contraction-initiating Ca^{2+} from the intracellular sarcoplasmic reticulum membrane network (Bers, 2002). The efficiency of RyR2 as a Ca^{2+}-release channel is underpinned by both tight regulation of gating and unusually high rates of Ca^{2+} translocation through the open channel (Williams et al., 2001). Altered RyR2 function underlies the occurrence of arrhythmia and sudden death in both inherited and acquired disease, and the channel is emerging as an important new therapeutic target (George and Lai, 2007; George et al., 2007; Hilliard et al., 2010).

Measurements of ion translocation and discrimination in individual RyR2 channels have established that although RyR2 is ideally selective for cations over anions, it is permeable to a wide range of inorganic divalent cations, inorganic monovalent cations, and organic monovalent cations. It would appear that high rates of Ca^{2+} movement through RyR2 are achieved at the expense of the high degree of discrimination displayed by cell surface K^+, Na^+, and Ca^{2+} channels (Williams et al., 2001).

The structural components of the pore-forming region (PFR) of K^+ channels and, as a consequence, the mechanisms by which these components regulate ion discrimination and translocation were revealed by the crystallization of prokaryotic channels (Doyle et al., 1998; Cordero-Morales et al., 2006). The enormous size of RyR2 (the functional channel is a homotetramer with each monomer containing in excess of 4,900 amino acids) and the lack of a prokaryotic analogue

S.A. Mason and C. Viero contributed equally to this paper.

Correspondence to Alan J. Williams: williamsaj9@cardiff.ac.uk

Abbreviations used in this paper: PFR, pore-forming region; *Sh*BP, *Shaker* B inactivation peptide; TAA, tetraalkylammonium; TBA, tetrabutylammonium; THexA, tetrahexylammonium; TPeA, tetrapentylammonium; WT, wild type.

The Rockefeller University Press $30.00
J. Gen. Physiol. Vol. 140 No. 3 325–339
www.jgp.org/cgi/doi/10.1085/jgp.201210851

currently preclude crystallization of the intact RyR2 tetramer. However, because of significant similarities in the primary and secondary structures of regions of RyR2 and the PFR of K^+ channels, it has been possible to construct a plausible analogy model of the RyR2 PFR based on a bacterial channel (KcsA) template (Welch et al., 2004). The model indicates that the putative RyR2 PFR and K^+ channels share several basic structural elements, and it appears likely that the two species of channel use similar fundamental strategies to allow ions to cross the permeability barrier created by the phospholipid bilayer. However, RyR2 is not a K^+ channel, and key features of the model highlight potential differences that could account for the unique features of ion handling that are characteristic of RyR2 and the other RyR isoforms. In the absence of detailed structural information, the analogy model provides us with a framework that can be used to test the involvement of domains or specific residues in RyR2 function. As an example, the model indicates that both the cytosolic and luminal entrances to the PFR will contain a high density of acidic residues, and the implication of this observation is that these regions could underlie the exceptionally high rates of cation translocation seen in RyR2. Consistent with this proposal, neutralization of specific residues at the luminal mouth of the PFR by alanine substitution resulted in reduced unitary conductance at subsaturating ion activities (Mead-Savery et al., 2009).

Another important prediction of the model is that the PFR of RyR2 will contain a water-filled cytosolic cavity. In K^+ channels, the walls of the cytosolic cavity are lined with predominantly hydrophobic residues of the inner helices of the PFR. In our RyR2 analogy model, equivalent hydrophobic residues are provided by the terminal transmembrane helix TM10 (Zorzato et al., 1990). In addition to lining the water-filled cytosolic cavity, hydrophobic residues of the K^+ channel inner helices have been identified as sites of interaction for blocking moieties including tetraalkylammonium (TAA) cations, local anesthetics, and inactivation peptides, ligands which, before the availability of detailed structural information, proved exceptionally useful as probes of the PFRs of K^+ channels (Zagotta et al., 1990; Choi et al., 1993; Valenzuela et al., 1995; Hille, 2001). Consistent with our assertion that RyR2 shares basic structural components with K^+ channels, all of these classes of molecule are effective blockers of RyR2 (Mead et al., 1998; West and Williams, 2007).

In this study, we describe novel investigations in which we have used large TAAs and *Shaker* B inactivation peptides (*Sh*BPs) as hydrophobic probes of the RyR2 PFR. By monitoring variations in blocking parameters arising from alterations in the hydrophobicity of both the blocking molecules and selected residues of the recombinant mouse RyR2 TM10, we have tested the proposal that these residues line the cytosolic cavity of the PFR of the channel.

The experiments described in this study provide important new information on the mechanisms and sites of interaction involved in TAA and *Sh*BP block of RyR2. In addition, our data reveal significant differences in mechanisms of block in RyR2 and K^+ channels that likely reflect structural specializations of the two PFRs that underlie their different physiological roles.

MATERIALS AND METHODS

TAA cations

TAA salts and standard chemicals, at the best available grade, were obtained from Sigma-Aldrich. Synthetic PE (1-palmitoyl-2-oleoyl-*sn*-glycero-3-phosphoethanolamine) was supplied by Avanti Polar Lipids, Inc.

Inactivation peptides

While maintaining a net charge of 3, we modified *Sh*BP hydrophobicity by residue substitution in the N terminus of the peptide. We have avoided residue substitution at and around leucine 7 as, although substitutions of this residue are likely to make significant changes to the hydrophobicity of the peptide, some studies have suggested that alterations in this region could bring about significant changes in structure that might themselves alter the effectiveness of the peptide as a blocker of K^+ channels (Fernandez-Ballester et al., 1995; Molina et al., 2008; Neira, 2009). For this reason, we have made relatively conservative substitutions that are less likely to alter the conformation of the peptide. A schematic representation of the peptide analogue sequences used in this study, *Sh*BP (MAAVAGLYGLGEDRQHRKKQ), a peptide less hydrophobic than *Sh*BP (LHBP, MAQVQGLYGLGEDRQHRKKQ), and two peptides more hydrophobic than *Sh*BP (MHBPI, MAVVAGLYGLGEDRQHRKKQ; and MHBPII, MAAVVGLYGLGEDRQHRKKQ) and a description of their synthesis and analysis can be found in Fig. S1. To compare the level of hydrophobicity of the different peptides, we attributed each a GRAVY (grand average of hydropathicity) score. A positive GRAVY value indicates a hydrophobic protein, whereas a negative value indicates a hydrophilic protein (Kyte and Doolittle, 1982). GRAVY values were determined using the ProtParam tool (Gasteiger et al., 2005).

Site-directed mutagenesis, expression of wild-type (WT) and mutant RyR2 cDNAs in HEK cells, and channel purification

Point mutations were introduced into TM10 (Zorzato et al., 1990) of mouse RyR2 by the overlapping extension method using polymerase chain reaction as described previously (Chen et al., 2002). HEK293 cells were grown in supplemented Dulbecco's modified Eagle's medium (Invitrogen) for 18 h in 100-mm-diameter tissue culture dishes seeded at a density of 10^6 per dish. Each dish was transfected and grown for 48 h with 12 µg of either WT or mutant RyR2 cDNA using Ca^{2+} phosphate precipitation. Cell pellets were solubilized for 1 h at 4°C using 0.6% CHAPS and 0.3% phosphatidylcholine at a protein concentration of 2 mg/ml. After a low-speed (14,000 *g*) spin, the solubilized supernatant was placed on top of a continuous (0–40%) sucrose gradient that was spun at 100,000 *g* for 17 h at 4°C. Sucrose gradients were separated into 2-ml fractions, and the density of the fractions was assessed using a 0–50% sugar refractometer (Bellingham & Stanley Ltd.) to identify fractions at ∼28% that contain functional RyR2 channels. Aliquots from these fractions were flash frozen in liquid nitrogen and stored at −80°C.

Planar phospholipid bilayers

Planar phospholipid bilayers were formed from a suspension of synthetic PE in 35 mg/ml *n*-decane by painting across a 200-µm-diameter hole in a partition separating the cis (0.5 ml) and trans (1.0 ml) chambers. The trans chamber was held at ground, and the cis chamber was clamped at potentials relative to ground. Current flow was measured using an operational amplifier as a current-voltage converter (Miller, 1982; Williams, 1995). Bilayers were formed in symmetrical solutions containing either 200 or 600 mM KCl and 20 mM HEPES titrated to pH 7.2 with KOH, resulting in solutions containing either 210 or 610 mM K^+ in both chambers. To measure single channel currents, aliquots of RyR2-containing fractions were added to the cis chamber, and channels were incorporated by imposing a KCl gradient (Sitsapesan and Williams, 1994). After incorporation, unincorporated channels and the osmotic gradient were removed by perfusion. RyR2 channels incorporate in a fixed orientation with the cytosolic face exposed to the cis chamber and the luminal face to the trans chamber (Sitsapesan and Williams, 1994). All experiments were performed at room temperature (22 ± 2°C).

Protocols used to monitor block

TAA cations. The blocking effects of tetrabutylammonium (TBA), tetrapentylammonium (TPeA), and tetrahexylammonium (THexA) were determined after their addition to the solutions at both the cytosolic and luminal faces of the channel at the concentrations indicated in the text. We have optimized the quantification of block in the WT channel by using experimental conditions that maximize open duration. This was achieved by monitoring function with high permeant ion concentrations (610 mM K^+) in the presence of 20–100 µM cytosolic EMD 41000, an analogue of isomazole shown previously to act via the caffeine-binding site on RyR2 (McGarry and Williams, 1994). Under these conditions, P_o is increased to ∼0.9 (Tanna et al., 1998) and the interaction of TAAs results in the occurrence of well-resolved reduced or subconductance states.

Identical conditions were used initially in experiments to establish the consequences of reducing TM10 residue hydrophobicity by alanine substitution. However, as explained in the Results, EMD 41000 did not significantly increase open times in all of the substituted channels. As a consequence, we have used ryanodine to maximize open times in the substituted channels (Mead et al., 1998). The interaction of ryanodine with the channel brings about a dramatic increase in P_o together with a reduction in conductance that reflects alterations in the affinity of the channel for some ions and altered relative permeabilities (Lindsay et al., 1994). We have assessed the consequences of ryanodine modification in the WT mouse RyR2 by comparing blocking parameters of TBA and TPeA in EMD 41000–activated and ryanodine-modified channels. The data shown in Fig. S3 demonstrate that ryanodine modification results in an equivalent reduction in the rate of association of both TAAs and that the very marked difference in the rates of dissociation of TBA and TPeA is retained in ryanodine-modified channels. These investigations demonstrate that although ryanodine modification may induce localized rearrangements in the helices of the PFR, the structural components making up this region of the channel are not altered.

ShBPs. We previously established that *Sh*BPs block K^+ translocation from the cytosolic face of RyR2 channels and that the kinetics of block are such that individual blocking events are resolved as brief transitions to levels indistinguishable from the normal closed level of the channel (Mead et al., 1998). To gain meaningful information on the mechanisms underlying block, it is essential that channel closing events that could contaminate block be minimized during the recording period. As outlined in the previous section, P_o values approaching 1.0 can be sustained in symmetrical 610 mM KCl plus up to 100 µM EMD 41000 (Tanna et al., 1998), and our initial experimental approach was to monitor the interactions of *Sh*BP, LHBP, MHBPI, and MHBPII with RyR2 under these conditions. However, preliminary experiments revealed that the peptides were ineffective at this high K^+ activity, an observation which is entirely consistent with the conclusion drawn in our earlier investigations (Mead et al., 1998), that electrostatic interactions make a major contribution to block of RyR2 by *Shaker* inactivation peptides. We observed no significant reduction in P_o after the addition of 20 µM *Sh*BP to the solution at the cytosolic face of ryanodine-modified channels in symmetrical 610 mM KCl (mean P_o in the absence of peptide, 0.91 ± 0.07 [n = 7]; mean P_o after the addition of *Sh*BP, 0.98 ± 0.01 [n = 5]). As a consequence, we have, as was the case in earlier investigations (Mead et al., 1998), monitored *Sh*BP interactions with individual RyR2 channels in symmetrical 210 mM KCl after modification with ryanodine.

Data acquisition and analysis

Current fluctuations of both EMD 41000–activated and ryanodine-modified channels were low-pass filtered at 5 kHz with an 8-pole Bessel filter and sampled at 20 kHz with a PCI-6036E A-D board (National Instruments) for acquisition using Acquire 5.0.1 (Bruxton). Single channel current amplitudes were measured directly on screen using Review 5.0.1 or from all-point histograms using TACx4.1.5 (Bruxton). Lifetimes of events in the EMD 41000–activated or ryanodine-modified open and blocked states were determined by 50% threshold analysis in sections of data with duration of at least 2 min (Mead and Williams, 2002). The methods used for the determination of parameters of block for TAAs and inactivation peptides are described in detail in the Supplemental text and Fig. S2.

Statistical analysis

Results were displayed and analyzed using the program Prism 5.02 (GraphPad Software). Unless otherwise stated, we applied unpaired *t* tests for analyzing the statistical significance of changes between one experimental condition and the corresponding control. Effects were regarded as significant when $P < 0.05$ (*, $P < 0.05$; **, $P < 0.01$; ***, $P < 0.001$). The results are expressed as mean values ± SEM. Normal distributions were assessed by the Kolmogorov-Smirnov test.

Online supplemental material

Fig. S1 shows the composition of the inactivation peptides used in this study, and the accompanying text provides details of the methods used in the production of the peptides and the characterization of their properties. Fig. S2 shows lifetime analysis of a representative ryanodine-modified RyR2 channel before and after the addition of *Sh*BP and demonstrates that the interaction of the peptide gives rise to several different populations of blocking event; the accompanying text describes the methods used to determine the blocking parameters of TAA cations and inactivation peptides in RyR2. Fig. S3 shows a comparison of the parameters of block of EMD 41000–activated and ryanodine-modified RyR2 channels by both TBA and TPeA and demonstrates that the overall differential between rates of dissociation of the two TAAs is maintained after ryanodine modification of the channel. Figs. S4 and S5 show, respectively, characterization of the concentration and voltage dependence of block of the WT ryanodine-modified recombinant RyR2 by the inactivation peptides used in this study; parameters of block derived from these characterizations are used to demonstrate the dependence of block on peptide hydrophobicity. Online supplemental material is available at http://www.jgp.org/cgi/content/full/jgp.201210851/DC1.

RESULTS

The influence of ligand hydrophobicity on block of WT recombinant RyR2

TAA cations. TAA cations have the general formula $(C_nH_{2n+1})_4N^+$, and increases in n raise both the hydrophobicity and size of the cation. To test the hypothesis that the hydrophobicity of TAA cations influences the kinetics of the blocking interaction, we have characterized the actions of TBA (n = 4), TPeA (n = 5), and THexA (n = 6).

All three TAAs block RyR2 when present in the solution at the cytosolic face of the channel with net current flow from the cytosolic to luminal side of the channel. Significantly, these blocking TAAs do not fully occlude the pore so that with the TAA bound, permeant ion translocation continues, albeit at a reduced rate. Individual blocking events can be resolved, and, as expected for a true partial blocking event, the residual current produced by each TAA varies linearly with holding potential, remaining a fixed proportion of the full open current (not depicted). Representative traces showing block by TBA, TPeA, and THexA are shown in Fig. 1.

In K^+ channels, it is well established that the kinetics of interaction of TAA cations are influenced by their hydrophobicity (Armstrong, 1971; French and Shoukimas, 1981; Choi et al., 1993; Zhou et al., 2001). Variation in the kinetics of TAA interaction with recombinant WT mouse RyR2 is demonstrated in Fig. 2 A, which shows the relationships between rates of TAA association and dissociation and cation hydrophobicity, expressed as the octanol/water partition coefficient (log P). The values of log P are those calculated by Rogers and Higgins (1973) and are based on the linear relationship between experimentally observed log P values for smaller TAAs and the number of carbon atoms in the cation. Although rates of TAA association (k_{on}) with the open channel change only slightly across the group, rates of dissociation of TAA show significant variation. We observe a dramatic (22-fold) decrease in k_{off} between TBA and TPeA

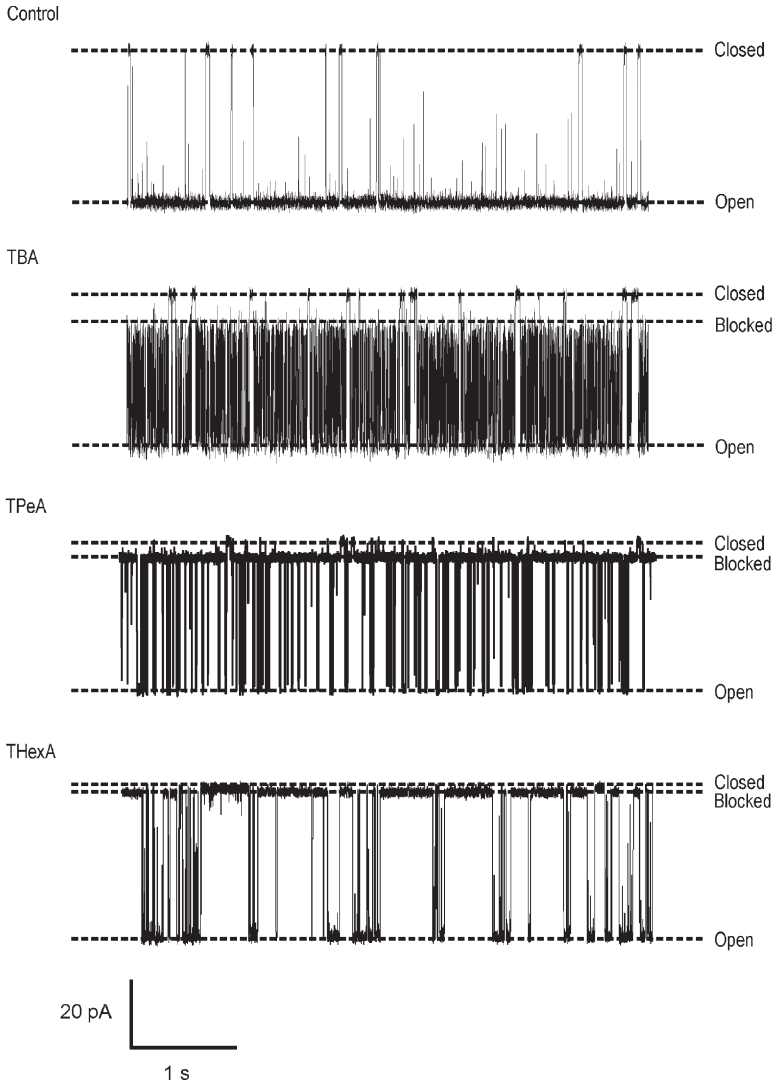

Figure 1. Large TAAs induce a characteristic partial block of K^+ current in RyR2 channels. Single channel recordings of purified, EMD 41000–activated RyR2 channels at a holding potential of 60 mV with 610 mM K^+ as the charge carrier. Addition of large TAAs (200 μM TBA, 100 μM TPeA, and 10 μM THexA) results in the occurrence of well-resolved blocking events.

followed by a much smaller (1.7-fold) decrease between TPeA and THexA. Together these differences contribute to a 69.5-fold increase in affinity between TBA and THexA (K_d TBA, 179.22 µM; THexA, 2.58 µM). Variations in rates of blocker dissociation are consistent with the involvement of hydrophobic interactions between the TAA and residues of the RyR2 PFR in the stabilization of the blocking cation, a situation reminiscent of the mechanisms of block by these cations in many K^+ channels (Hille, 2001). The relatively small change in k_{off} observed between TPeA and THexA indicates that the hydrophobic component of TAA stabilization in RyR2 is saturable.

An additional novel observation that arises from this study is that the TAA-induced residual current in RyR2 is dependent on the size of the blocking cation and decreases linearly as the radius of gyration of the cation (determined as the mean distance from the center of mass of the cation in molecular dynamics simulations) is increased (Fig. 2 B). Extrapolation of this relationship indicates that residual current would be zero, indicating occlusion of the channel, with a TAA with a radius of gyration of ∼5 Å or greater.

ShBPs. We have quantified block of WT recombinant ryanodine-modified RyR2 channels by *Sh*BPs of differing hydrophobicity (see Fig. S1 for residue distribution). The WT peptide *Sh*BP (MAAVAGLYGLGEDRQHRKKQ) has a distinct hydrophobic N-terminal domain and a C-terminal domain carrying a net positive charge. The relative hydrophobicity of *Sh*BP, as assessed by the GRAVY score of hydropathicity, was −0.87 for the whole peptide and 1.70 for the hydrophobic region alone. We rendered *Sh*BP less hydrophobic by replacing two alanine residues with glutamine residues at positions 3 and 5, yielding a mutant peptide, MAQVQGLYGLGEDRQHRKKQ (LHBP). The relative hydrophobicity of LHBP was −1.40 for the whole peptide and 0.64 for the hydrophobic region. To produce peptides in which the overall hydrophobicity was increased relative to *Sh*BP, we replaced alanine residues either in position 3 or 5 by a valine, resulting in MAVVAGLYGLGEDRQHRKKQ (MHBPI, GRAVY score −0.75 for the whole peptide and 1.94 for the hydrophobic region) and MAAVVGLYGLGEDRQHRKKQ (MHBPII, GRAVY score −0.75 for the whole peptide and 1.94 for the hydrophobic region). All of the peptides investigated had a net charge of 3.

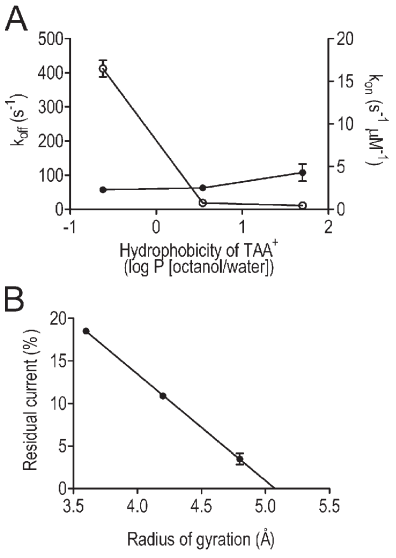

Figure 2. Parameters of TAA block of RyR2 channels. (A) Rates of TAA association (closed circles, k_{on}) and dissociation (open circles, k_{off}) were determined at 60 mV and are plotted against cation hydrophobicity (monitored as the octanol/water partition coefficient). (B) The residual current after the interaction of 200 µM TBA, 100 µM TPeA, and 10 µM THexA was determined at 60 mV and expressed as a percentage of full open current and is plotted against the radius of gyration of the three TAAs (determined using SYBYL; Tripos). (A and B) Data are plotted as mean values (±SEM; $n = 4$ for TBA and THexA and $n = 5$ for TPeA).

In all cases, addition of peptide to the solution at the cytosolic face of the ryanodine-modified channel resulted in the occurrence of blocking events to a level indistinguishable from the normal closed level (Fig. 3 A). The probability of block by all four peptides varies with concentration (rates of association are linearly dependent on concentration, whereas rates of peptide dissociation are concentration independent [Fig. S4]). Similarly, block by all peptides varies with holding potential (in all cases, both rates of association and dissociation are voltage dependent [Fig. S5]).

The consequences of altering the hydrophobicity of *Sh*BPs on the kinetics of their interaction with individual recombinant mouse RyR2 channels are summarized in Fig. 3 B, in which parameters of block are plotted against the GRAVY score of the N-terminal domain of the peptide. As is the case with the TAA cations, the effect of varying blocker hydrophobicity is seen predominantly as a change in the rate of *Sh*BP dissociation, with little or no effect on the rate of association. Rates of dissociation vary linearly with the peptide GRAVY score. The value of $1/T_B$ for MHBPI is 3.1-fold lower than that of LHBP, and these differences underlie a 2.4-fold difference in affinity between these peptides (K_d LHBP, 65.90 µM; MHBPI, 27.79 µM). The small difference between the parameters of MHBPI and MHBPII, which have the same overall GRAVY score, presumably reflects local structural differences in the two peptides.

The data described in this section establish that the probability of block of the RyR2 channel by both TAA cations and *Sh*BPs is influenced by the hydrophobicity of the blocking molecule. The magnitude of the changes seen with the two classes of blocker is very different; however, in both cases the rate of blocker association with RyR2 is independent of the hydrophobicity of the molecule, whereas the rate of blocker dissociation is reduced by increased hydrophobicity.

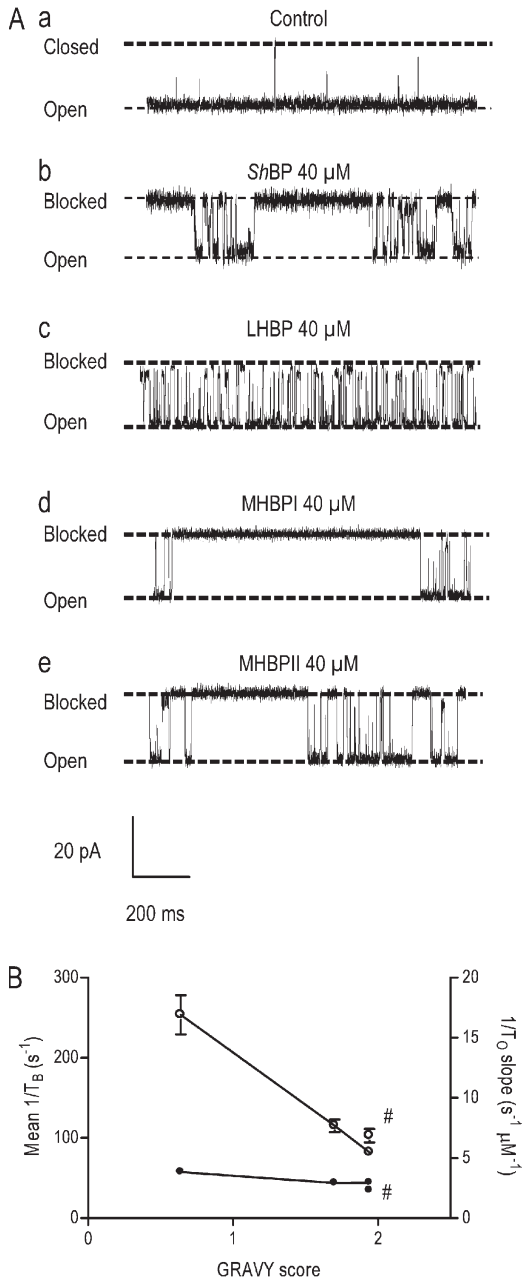

Figure 3. Block of RyR2 channels by *Sh*BPs. (A) Representative recordings of individual ryanodine-modified RyR2 channels in symmetrical 210 mM KCl (a) and after the addition of 40 µM *Sh*BP (b), LHBP (c), MHBPI (d), and MHBPII (e) to the solution at the cytosolic (cis) side of the channel. In all cases, the holding potential was 50 mV. Closed, open, and blocked levels are indicated by dashed lines. (B) Rates of peptide association ($1/T_o$ slope [per second/micromolar]; closed circles) and rates of peptide dissociation (mean $1/T_B$ [per second]; open circles) are plotted against the GRAVY score of the hydrophobic portions of the four peptides: ShBP ($1/T_o$ $n = 3$–11, $1/T_B$ $n = 3$–13), LHBP ($1/T_o$ $n = 3$–9, $1/T_B$ $n = 4$–8), MHBPI ($1/T_o$ $n = 3$–7, $1/T_B$ $n = 3$–6), and MHBPII ($1/T_o$ $n = 4$–10, $1/T_B$ $n = 4$–9). Data are plotted as mean values (±SEM). As MHBPI and MHBPII have the same GRAVY score, MHBPII-related values are signified by "#."

These observations indicate that hydrophobic interactions are involved in the stabilization of both classes of blocking molecule in RyR2.

Identification of the site or sites of TAA and *Sh*BP interaction

Blocking TAA cations and inactivation peptides interact with residues of helices that line the cytosolic vestibules of K^+ channels. Crystallization of K^+ channel–TAA complexes has revealed the identity of residues that contribute to the binding site for these cations (Lenaeus et al., 2005; Faraldo-Gómez et al., 2007; Yohannan et al., 2007). Faraldo-Gómez et al. (2007) describe TBA as a "4-fold cross lying parallel with the plane of the membrane within the cytosolic cavity of KcsA." The center of the TBA cross is located in line with the central axis of the pore at the entrance to the selectivity filter, and the blocking molecule is stabilized by interactions of its four hydrocarbon arms with hydrophobic residues (I100 and F103 in KcsA) of each of the helices lining the cavity. In this location, TBA fully occludes the pore of the channel, preventing translocation of K^+. It is also established that TAAs and inactivation peptides share sites of interaction and common mechanisms of block in K^+ channels (Zhou et al., 2001), and the identity of hydrophobic residues involved in the stabilization of both classes of molecule has been investigated by directed residue substitution (Choi et al., 1993; Zhou et al., 2001).

Our analogy model of the RyR2 PFR identifies TM10 as the helix lining the cytosolic cavity and equivalent to the inner helix of the K^+ channel PFR (Welch et al., 2004),

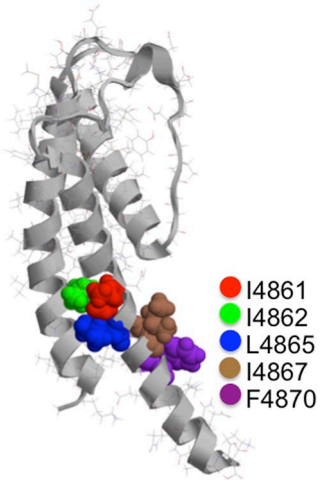

Figure 4. Location of hydrophobic residues in the proposed cytosolic cavity–lining helix (TM10) of RyR2. The figure shows one monomer of the Welch et al. (2004) model of the RyR2 PFR. The luminal entrance to the pore is at the top of the structure, and the cytosolic entrance is at the bottom. The hydrophobic residues of TM10 investigated in this study are highlighted, shown in space-fill, and identified in the key. Molecular graphics were rendered with Ras Top 2.0.2 software.

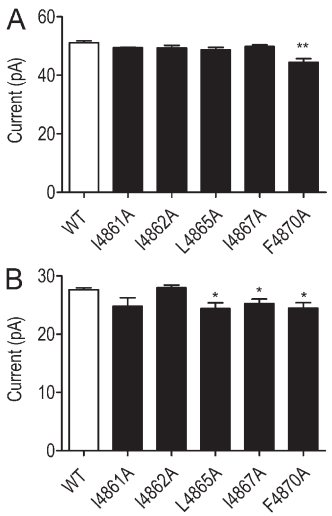

Figure 5. Current amplitudes in WT and residue-substituted channels. (A) Current amplitude of WT and TM10 alanine-substituted RyR2s at 60 mV after activation by 20 μM EMD 41000. (B) Equivalent current amplitudes after channel modification by 1 μM ryanodine. Data are plotted as mean values (±SEM; n = 4–7; *, $P < 0.05$; **, $P < 0.01$).

and we have investigated the potential contribution of RyR2 TM10 residues to TAA and *Sh*BP blocker stabilization. TM10 contains a motif analogous to the gating hinge motif present in the inner helices of many K^+ channels (GXXXXA/G; ^{4864}GLIIDA^{4869} in mouse RyR2; Jiang et al., 2002; Shealy et al., 2003), and aligning the residues of TM10 with the inner helix of KcsA using ^{4864}G and ^{99}G as reference points (underlined) highlights the residues of interest for investigation:

mouse RyR2 TM10, ^{4858}LLAIIQGLIIDAFGE^{4872};
KcsA inner helix, ^{93}VVVMVAGITSFGLVT^{107}.

The location of these residues within our analogy model of the RyR2 PFR is shown in Fig. 4. To identify TM10 residues that are potentially involved in TAA and *Sh*BP block in RyR2, we have made a series of channels in which individual hydrophobic residues of the TM10 sequence shown above (isoleucine, leucine, and phenylalanine) have been replaced with alanine.

Properties of TM10 mutant RyR2 channels

All substituted RyR2 channels were expressed at levels equivalent to the WT channel in HEK293 cells (Wang et al., 2003); however, L4858A, L4859A, and I4866A failed to form functional channels, as assessed by the ability of caffeine to release stored Ca^{2+} in intact transfected HEK293 cells and the ability of isolated ER membranes to bind significant quantities of [^{3}H]ryanodine (Wang et al., 2003). As a result, these RyR2 channels could not be investigated further. The remaining substituted RyR2 channels (I4861A, I4862A, L4865A, I4867A, and F4870A) were purified as described in Materials and methods, and their single channel properties were characterized after incorporation into planar phospholipid bilayers. The ion-handling properties of these channels were not altered dramatically by residue substitution. The single

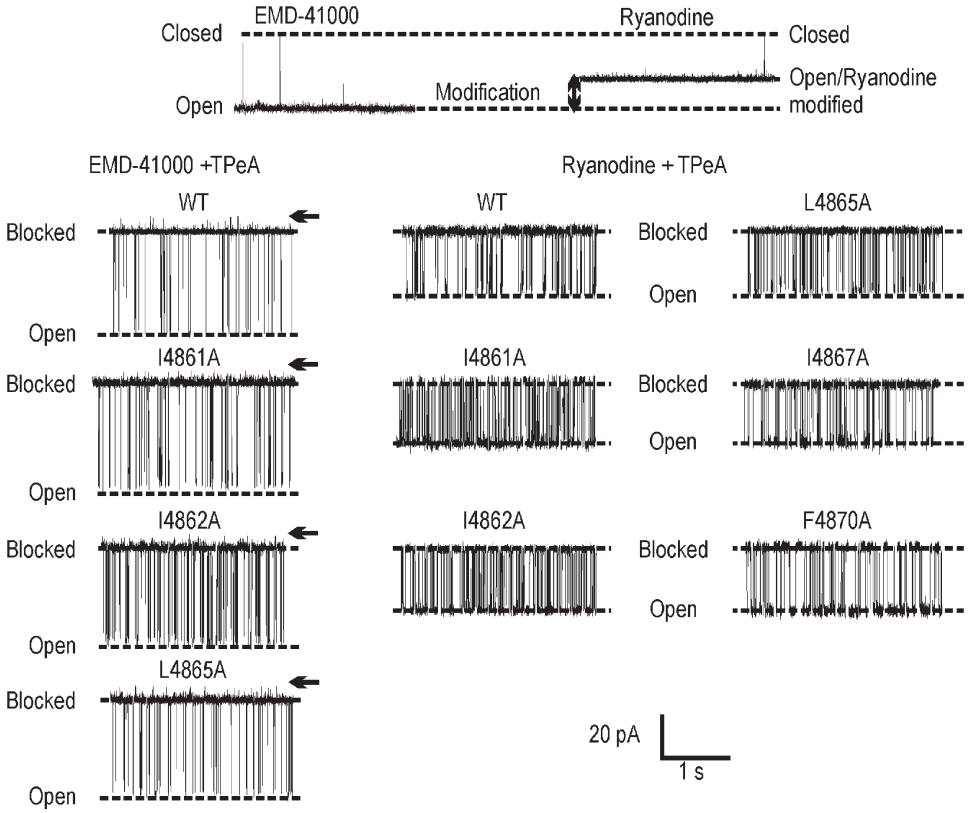

Figure 6. TPeA block of EMD 41000–activated and ryanodine-modified WT and substituted channels. The top panel shows representative traces of RyR2 in the absence of TPeA after addition of 20 μM EMD 41000 (left) and 1 μM ryanodine (right). The bottom left panel shows block of the WT and alanine-substituted EMD 41000–responsive channels by 100 μM TPeA at 60 mV. Closed levels are indicated by arrows. The bottom right panel shows representative traces of block of WT and substituted channels by 100 μM TPeA at 60 mV after modification by 1 μM ryanodine.

channel K^+ conductance of I4861A, I4862A, L4865, and I4867A was indistinguishable from that of the WT RyR2s, whereas conductance of F4870A was reduced by ~10% (Fig. 5 A).

During our initial characterization of substituted RyR2 channels, it was apparent that in only three (I4861A, I4862A, and L4865A) did EMD 41000 drive P_o to values approaching 1.0. We have quantified block by TPeA in these three EMD 41000–activated substituted channels and in all five ryanodine-modified channels. To characterize the effects of residue substitution on block by *Sh*BP, we have monitored the actions of the most effective peptide (MHBPI) in all five ryanodine-modified channels.

The consequences of the modification of substituted channels by ryanodine are shown in Fig. 5 B. The amplitude of the ryanodine-modified open state of I4861A and I4862A is not significantly different from that of the WT channel, whereas in L4865A, I4867A, and 4870A, conductance of the ryanodine-modified state is ~10% lower than that of the WT modified channel.

Block of TM10-substituted recombinant RyR2 channels

TAA cations. Its high affinity and clearly resolved residual current make TPeA an ideal probe with which to monitor alterations in blocking parameters resulting from the substitution of hydrophobic residues in TM10 of RyR2. Traces showing block of the open state of the channel are shown in Fig. 6.

As with the WT channel, TPeA interaction with EMD 41000–activated I4861A, I4862A, and L4865A RyR2 is characterized by block to a level clearly distinguishable from the closed level (Fig. 6, left). In the presence of TPeA, the amplitudes of the full open states of all three substituted channels are indistinguishable from that of the WT channel, as are the blocker-induced residual currents in I4862A and L4865A. The residual current in I4861A is slightly lower than the equivalent current in the WT RyR2 (Fig. 7). These observations support the proposal that the replacement of I4861, I4862, or L4865 with alanine does not produce major disruption of the structure of the PFR.

The interaction of ryanodine produces the characteristic increase in P_o and reduction in unitary conductance in all five substituted RyR2s. After modification by ryanodine, TPeA blocks both the WT and substituted channels to a level indistinguishable from the closed state (Fig. 6, right).

Substitution-dependent variations in block of EMD 41000–activated channels. Blocking parameters for EMD 41000–activated channels are shown in Fig. 8. When compared with the WT channel, the probability of block by TPeA is reduced significantly in both I4861A and I4862A but not in L4865A (Fig. 8 A). Rates of TPeA association are unaffected by any of the substitutions (Fig. 8 B), but all three substitutions led to significantly increased rates of TPeA dissociation, with the most dramatic effect seen in I4862A (Fig. 8 C). Alterations in rates of dissociation resulted in significant decreases in TPeA affinity in I4861A and I4862A (Fig. 8 D).

Substitution-dependent variation in block of ryanodine-modified channels. Parameters for the block of WT and substituted ryanodine-modified channels by 100 µM TPeA are shown in Fig. 9. The open probability of all substituted channels is reduced by the addition of TPeA. In all cases, the magnitude of block is lower than that seen in the WT RyR channel (Fig. 9 A). All substituted RyR2 channels exhibited a significant increase in k_{off} when compared with the WT channel (Fig. 9 B). The scale of the effects of residue substitution on k_{off} was comparable with those seen in EMD 41000–activated

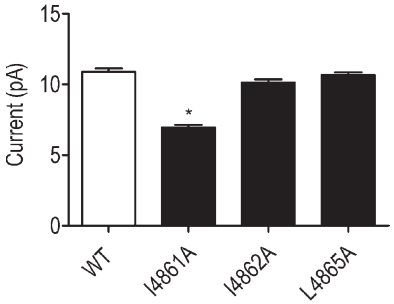

Figure 7. Residual current in WT and substituted EMD 41000–activated channels. Single channel current amplitudes of TPeA-blocked states monitored at 60 mV in the presence of 100 µM blocker. Data are plotted as mean values (±SEM; n = 4–7; *, $P < 0.05$).

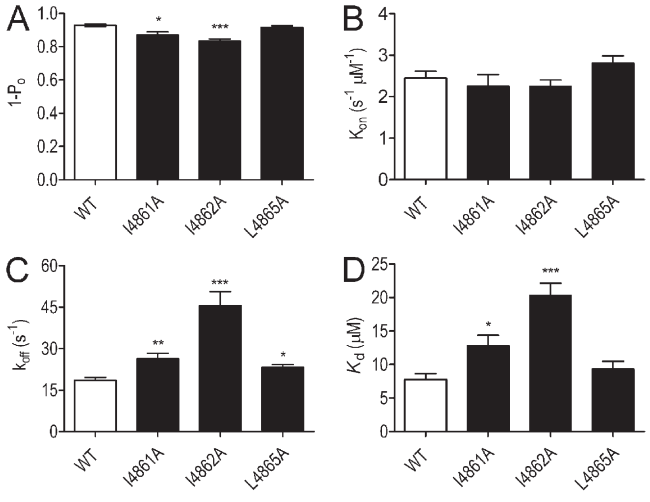

Figure 8. The probability of block ($1 - P_o$), rates of association/dissociation (k_{on}/k_{off}), and the affinity (K_d) of TPeA in EMD 41000–activated WT and substituted RyR2 channels. (A–D) Blocking parameters were determined at 60 mV in the presence of 100 µM TPeA. Data are plotted as mean values (±SEM; n = 5–7; *, $P < 0.05$; **, $P < 0.01$; ***, $P < 0.001$).

channels (compare Fig. 8 C with Fig. 9 B). In contrast to the situation in EMD 41000–activated channels, where residue substitution produced no significant changes in the rate of TPeA association, rates of TPeA association with substituted channels were reduced significantly in some (I4861A, I4867A, and F4870A) of the ryanodine-modified RyR2s (Fig. 9 C). As a result of these changes in rates of association and dissociation, residue substitution produced a significant reduction in TPeA affinity in all five substituted channels (Fig. 9 D).

ShBPs. The traces shown in Fig. 10 demonstrate that MHBPI is an effective blocker of all of the substituted ryanodine-modified RyR2 channels. As in the WT channel, the majority of blocking events are to a level indistinguishable from the normal closed level of the channel, but some incomplete or subconductance events are seen in all substituted channels. Parameters of MHBPI block of WT and substituted channels are shown in Fig. 11. The probability of block by MHBPI was reduced by substitution with alanine of either I4862 or L4865; alanine substitution for I4861, I4867,

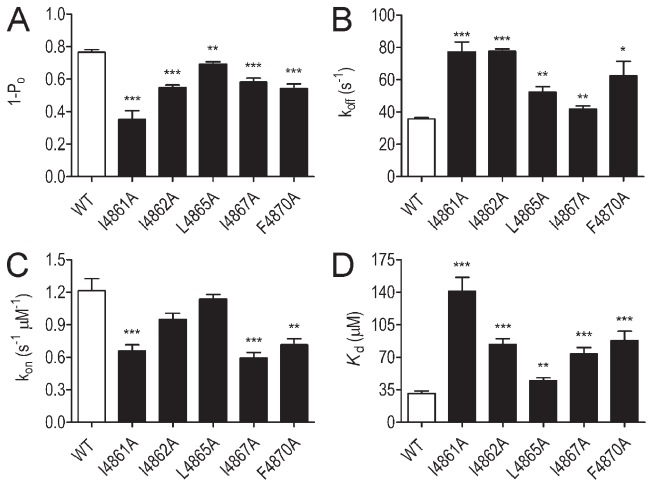

Figure 9. The probability of block ($1 - P_o$), rates of association/dissociation (k_{on}/k_{off}), and the affinity (K_d) of TPeA in ryanodine-modified WT and substituted RyR2 channels. (A–D) Blocking parameters were determined at 60 mV in the presence of 100 µM TPeA. Data are plotted as mean values (±SEM; $n = 5–8$; *, $P < 0.05$; **, $P < 0.01$; ***, $P < 0.001$).

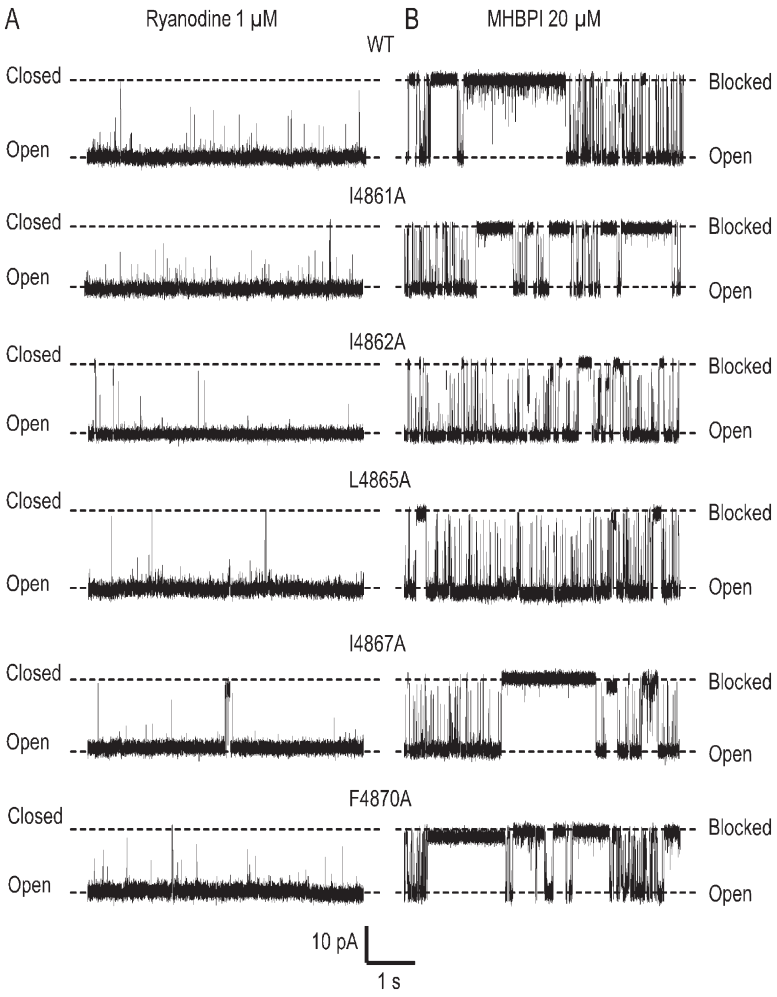

Figure 10. Effect of lowering the hydrophobicity of TM10 residues on the block of ryanodine-modified RyR2 channels by MHBPI. Representative single channel traces at a holding potential of 50 mV in symmetrical 210 mM KCl. MHBPI was applied to the cytosolic (cis) side of the RyR2 channels. Closed, open, and blocked levels are indicated by dashed lines. In each case, A shows representative activity of a ryanodine-modified channel before application of 20 µM MHBPI. B shows activity of the same channel after addition of the peptide.

and F4870 produced no significant alteration (Fig. 11 A). The reduced probability of block in I4862A resulted from a significant reduction in the rate of blocker association (Fig. 11 B). As demonstrated above, alanine substitution of I4861, I4862, L4865, I4867, and F4870 resulted in significant increases in the rate of TPeA dissociation from RyR2. In contrast, none of these substitutions increased the rate of dissociation of MHBPI, with the only significant alteration being a reduction in the rate of peptide dissociation in I4861A (Fig. 11 C). Overall, these data do not indicate that the reduction of the hydrophobicity of individual residues in RyR2 TM10 produces a significant destabilization of the bound *Sh*BP.

Variations in ShBP blocking parameters in response to increased lumen to cytosol K^+ flux. Does the lack of effect of TM10 residue substitution on peptide stabilization suggest that the site of *Sh*BP interaction is not within the conduction pathway of RyR2? We have used an alternative approach to assess a potential site of peptide interaction within the cytosolic vestibule of RyR2 by monitoring blocker–peptide interaction with increasing luminal (trans) to cytosolic (cis) K^+ gradients across the channel, a strategy which would be expected to destabilize or "knock off" blocking peptide if it is bound within the conduction pathway. A similar approach has been used to identify sites of interaction within the conduction pathway of a Ca^{2+}-dependent K^+ channel for *Sh*BP (Foster et al., 1992).

Block of WT RyR2 by *Sh*BPs and mutant peptides was monitored in symmetrical 210 mM KCl and then after the addition of 3 M KCl to the trans chamber to raise the concentration at the luminal side of the channel to 620 mM. In Fig. 12, rates of peptide association and dissociation are shown normalized to these rates in symmetrical 210 mM KCl. The increase in luminal to cytosolic K^+ flux significantly reduced the rate of *Sh*BP and MHBPII association (Fig. 12 A).

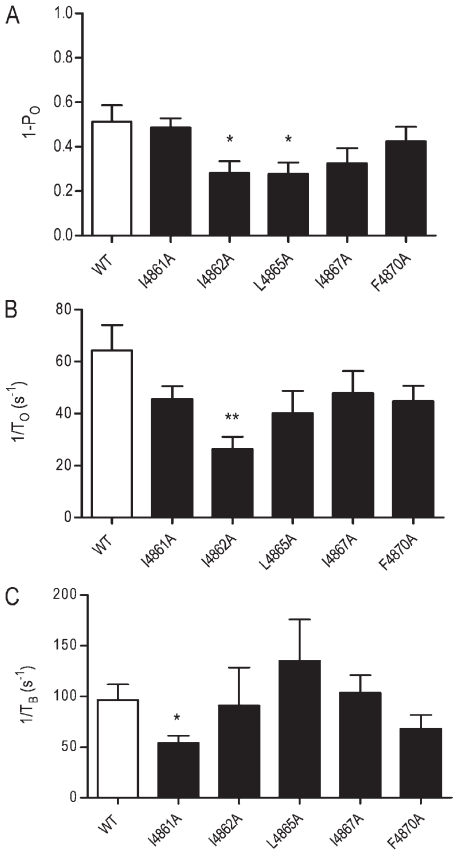

Figure 11. Analysis of the parameters of MHBPI block after alanine substitution of TM10 residues. (A–C) Parameters of block were determined for WT and alanine-substituted ryanodine-modified channels induced by 20 µM MHBPI at a holding potential of 50 mV in symmetrical 210 mM KCl. Data are plotted as mean ± SEM for between five and eight channels. When significant differences occur between the WT parameter and that of the substituted channel, this is indicated by asterisks (*, $P < 0.05$; **, $P < 0.01$).

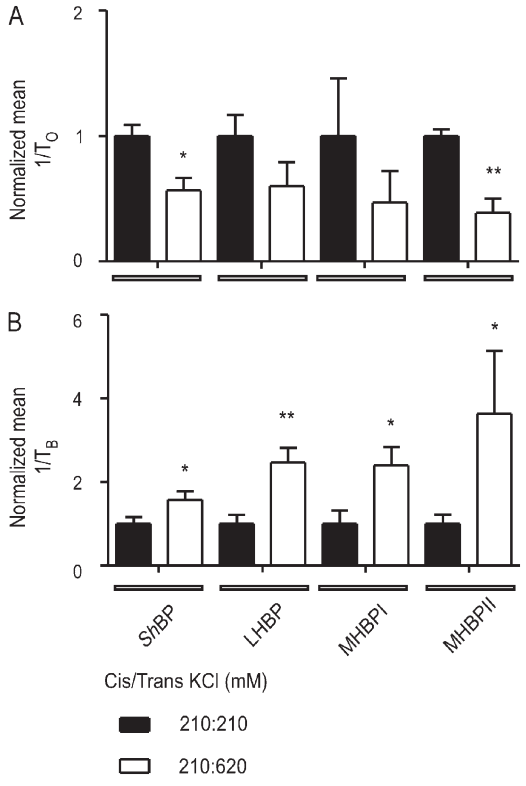

Figure 12. Destabilization of bound peptide analogues by increased luminal to cytosolic K^+ flux through ryanodine-modified RyR2 channels. (A) Normalized values of the pooled rates of association ($1/T_o$) for 20 µM *Sh*BP, 85 µM LHBP, 45 µM MHBPI, and 45 µM MHBPII monitored at 50 mV in either symmetrical 210 mM KCl or with 210 mM KCl in the cis chamber and 620 mM KCl in the trans chamber. (B) Normalized values of the pooled rates of dissociation ($1/T_B$) under the same conditions. Data are plotted as mean ± SEM for between three and eight channels. Each individual value (for 210:210 and 210:620) was normalized to the mean value of the 210:210 data for each peptide. Where differences between values obtained in 210:210 and 210:620 reached statistical significance, these are indicated by asterisks (*, $P < 0.05$; **, $P < 0.01$).

The rate of peptide dissociation was increased significantly in all cases by raised luminal to cytosolic K^+ flux (Fig. 12 B). Increased rates of dissociation and decreased rates of association in response to increased luminal to cytosolic K^+ flux indicate that the likely site of blocker–peptide interaction is within the conduction pathway of the RyR2 PFR.

DISCUSSION

In this study, we tested the proposal that, as is the case in K^+ channels, the RyR2 PFR contains a cytosolic cavity lined with transmembrane helices (TM10). To carry out this investigation, we have evaluated the hypotheses that (a) the blocking reactions of large TAA cations and *Sh*BPs in the RyR2 channel involve hydrophobic interactions and (b) these interactions occur between the blocking molecules and hydrophobic residues of TM10 helices that line the cytosolic cavity of the RyR2 PFR model.

New information on mechanisms of block of WT RyR2

TAA cations. The intracellular binding site for TAA cations in K^+ channels is located within the cytosolic cavity of the channel, with these cations stabilized by interactions with specific hydrophobic residues contributed by each of the four inner helices lining the cytosolic cavity. In KcsA, individual blocking events, to a level indistinguishable from the closed state, are clearly resolved, indicating that with the blocker in place, the conduction pathway of the channel is completely occluded (Faraldo-Gómez et al., 2007).

TAA cations are also blockers of RyR2. In contrast to K^+ channels, TAAs are only effective from the cytosolic face of the RyR2 channel, and the site of interaction of the TAA in RyR2 is dictated by the size and properties of the blocking cation. Determinations of the voltage dependence of TAA block in RyR2 indicate there to be three possible blocking sites (Williams et al., 2001): one occupied by tetramethylammonium (TMA), another occupied by TEA and tetrapropylammonium (TPrA), and a third occupied by the larger TAAs, TBA, TPeA, and, as demonstrated in this study, THexA.

A comparison of TAA blocking parameters in K^+ channels and RyR2 provides new insights into the respective mechanisms of block and thus the nature of the cytosolic sites of interaction within the two families of channel. In a recent publication (Faraldo-Gómez et al., 2007), it was reported that in K^+ channels, rates of TBA association were generally within the range 10^3–10^7/s/M, and the k_{on} determined here for TBA in RyR2 (2.3×10^6/s/M) is within this range. Rates of TBA dissociation from K^+ channels are quoted to be within the range 10–200/s; however, the k_{off} measured here for TBA from RyR2 is significantly higher (412/s). This, together with the observation that TAA block of RyR2 does not result in complete occlusion of the pore indicates that although TAA block in RyR2 and K^+ channels is superficially similar, the mechanisms underlying block must be significantly different.

Crystallization of K^+ channel–TBA complexes has revealed that the blocking cation is held parallel with the plane of the membrane in the cytosolic cavity of the channel at the entrance to the selectivity filter (Faraldo-Gómez et al., 2007). Stabilization involves van der Waals interactions within a ring of hydrophobic residues provided by each of the helices lining the cavity (I100 and F103 in KcsA) and electrostatic interactions with threonines at the base of the selectivity filter (T75 in KcsA).

In the absence of high-resolution structural information for RyR2, our analogy model of the PFR suggests that this region of the channel is likely to share basic structural components with K^+ channels, including a water-filled cavity at the cytosolic entrance to a selectivity filter (Welch et al., 2004). However, residual current with the TAA bound in RyR2 indicates that the blocking cation cannot be stabilized across the entrance to the selectivity filter as it is in K^+ channels. Consistent with this proposal, the spacing of residues at the entrance to the selectivity filter from the cytosolic cavity is significantly larger in the RyR2 model than in K^+ channels (Welch et al., 2004), indicating that the mechanism used to stabilize TBA in KcsA is not available in RyR2. The demonstration that increases in size and hydrophobicity of the large blocking TAAs bring about both a decrease in residual current and reductions in rates of blocker dissociation provides clues toward an understanding of both the mechanism of block and the location and make-up of the site of interaction within RyR2. A TAA immobilized in the cytosolic cavity will not fully obstruct the pore but will introduce an additional energy barrier to be overcome by a permeant cation. This barrier will have both an electrostatic and a steric component. As the electrostatic component of the barrier does not change, the incremental reduction in residual current seen with TBA, TPeA, and then THexA indicates that increasing bulk of the TAA progressively occludes the conduction pathway of the RyR2 channel. Variations in rates of TAA dissociation are consistent with stabilization by hydrophobic interactions. Therefore, it is logical to propose that, rather than being held at the axis of the pore, large blocking TAAs are stabilized at or near the wall of the cytosolic cavity of the RyR2 PFR by interactions involving hydrophobic residues of TM10. This site should be at a location where the conduction pathway would be occluded with a TAA of radius of gyration ≥ 5 Å in place. The approximate equivalence in values of k_{off} for TPeA and THexA likely indicates that all available TM10 residues that contribute to the stabilization of TAAs are involved in the interaction of TPeA and that no more can be recruited when the size and hydrophobicity of the blocking cation are increased further.

The data presented in Fig. S3 demonstrate that the contribution of hydrophobic interactions to TAA stabilization in RyR2 is retained after modification by ryanodine; however, the nature of block is altered. Rather than partially obstructing the conduction pathway, with ryanodine bound both TBA and TPeA completely occlude the RyR2 pore. It has been proposed that the high affinity binding of ryanodine induces a conformational change or stabilizes an intermediate open conformation of the RyR2 conduction pathway (Tanna et al., 2003). The altered profile presented to ions then accounts for the documented changes in ion handling (Lindsay et al., 1994). If the physical manifestation of the conformational adjustment is that the diameter of the conduction pathway is reduced at some point along its length, this could explain how a large TAA that only partially occludes the pore in the absence of ryanodine fully obstructs ion movement when bound at the same site in the ryanodine-modified channel.

ShBPs. Our earlier and current investigations have established that the *Sh*BPs are only effective blockers of RyR2 when present at the cytosolic face of the channel. The demonstration that block by these peptides is sensitive to transmembrane voltage and that rates of peptide association and dissociation are influenced by increased luminal to cytosolic K^+ flux indicates that, as is the case in K^+ channels, block of RyR2 results from the direct occlusion of the conduction pathway of the channel by the peptide.

Are the mechanisms of block equivalent in K^+ channels and RyR2? Inactivation peptide block of K^+ channels involves an initial electrostatic interaction between the C-terminal region of the peptide and residues outside the PFR. Pore occlusion occurs when the N-terminal domain of the elongated peptide enters the cytosolic cavity and is stabilized by hydrophobic interactions between residues of the peptide and residues of the helices lining the cavity (Murrell-Lagnado and Aldrich, 1993; Zhou et al., 2001). Similarly, our data indicate that block of RyR2 has both hydrophobic and electrostatic components. The current investigation has established that the rate of blocking peptide dissociation from RyR2 is determined by the hydrophobicity of its N-terminal portion, and in an earlier investigation we demonstrated that the rate of peptide association was dependent on the positive charge of the C-terminal region (Mead et al., 1998). Although differences in experimental conditions and the primary structure of the inactivation peptides used mean that it is not possible to make quantitative comparisons of all components of block, we can evaluate the contribution of peptide charge to block of RyR2 and K^+ channels. The kinetics of interaction of *Sh*BP (net charge 3) has been compared with that of a modified *Sh*BP (net charge 7) in *Shaker* (Murrell-Lagnado and Aldrich, 1993), Ca^{2+}-activated K^+ (K_{Ca}) channels (Toro et al., 1994), and RyR2 (Mead et al., 1998). Relative rates of association of these peptides differ wildly. An increase in net charge of 4 results in a 30-fold increase in *Shaker*, a 10-fold increase in K_{Ca}, but a 500-fold increase in RyR2. Interestingly, although this change in charge has essentially no influence on the relative rates of peptide dissociation from *Shaker* (Murrell-Lagnado and Aldrich, 1993), it induces a 10-fold decrease in RyR2. These observations suggest that although *Sh*BP block involves both electrostatic and hydrophobic interactions in both RyR2 and K^+ channels, peptide charge plays a significantly more important role in block of RyR2 than it does in K^+ channels. This in turn could reflect a high density of acidic residues at the entrance of the RyR2 cytosolic cavity (Welch et al., 2004).

Stabilization by hydrophobic interactions and the identification of blocker-stabilizing residues in RyR2

Our data establish that hydrophobic interactions contribute to the stabilization of blocking TAA cations and *Sh*BPs in the WT RyR2 channel. The replacement of hydrophobic residues in TM10 with alanine does not cause major disruption to ion handling. In all cases, the conductance of the full open state and the ryanodine-modified state were within 10% of the WT RyR2.

TAA cations. Intermolecular interactions, such as those demonstrated to stabilize TAAs in K^+ channels, arise from instantaneous dipole-induced dipole forces (London dispersion forces) between the carbon and hydrogen atoms of the arms of the TAA and equivalent atoms in hydrophobic residues of the PFR (Faraldo-Gómez et al., 2007). The strength of these forces is dependent on the size and shape of the interacting molecules and their proximity. Substitution of an interacting residue by alanine is likely to affect all three of these factors.

If, as we propose, large TAA cations are stabilized in the cytosolic cavity of the PFR by interactions with hydrophobic residues of TM10, it is probable that dipole-induced dipoles will occur within several residues of one or more helix: some between the TAA and residues and others between residues. The total number recruited and the resulting stabilizing force would then rise as the size of the TAA is increased. Rather than being held at the axis of the PFR by interactions with specific residues, as is the case in K^+ channels, we envisage large TAAs stabilized off-center by hydrophobic interactions with several residues of the cavity-lining helices. If this were the case, substitution of individual bulky hydrophobic residues with alanine would be expected to lower the interacting forces between the TAA and the PFR, with the scale of effect on the rate of TAA dissociation dependent on the contribution of individual hydrophobic residues to the overall stabilizing

force. In contrast to the situation in K^+ channels, the lowering of the hydrophobicity of an individual residue in RyR2 would not be expected to destabilize TAAs spectacularly as the majority of the contributing residues remain in place.

Our data are consistent with this picture. In both the EMD 41000–activated and ryanodine-modified channels, TM10 hydrophobic residue substitution by alanine produces significant increases in the rate of TPeA dissociation, indicating that all of these residues contribute to a greater or lesser degree to TAA stabilization in RyR2. Although quantitatively similar, the relative effects of substitution of I4861, I4862, and L4865 on k_{off} are not identical in the EMD 41000–activated and ryanodine-modified channels. This suggests that the ryanodine-dependent change in conformation of the PFR alters the local distribution of dipole-induced dipoles and thus the relative contribution of these residues to TPeA stabilization.

The ryanodine-dependent conformational change also results in some differences in the rate of TPeA association with the PFR. Alanine substitution of I4861, I4862, and L4865 produces no change in TPeA k_{on} in EMD 41000–activated channels. In ryanodine-modified channels, TPeA k_{on} is unaffected by alanine substitution of I4862 and L4865 but is reduced in I4861A. Similarly, the k_{on} for TPeA is reduced relative to the WT channel in I4867A and F4870A, substitutions which we were unable to examine in EMD 41000–activated channels. In the ryanodine-modified conformation of the RyR2 PFR, alanine substitution of some TM10 residues likely produces local changes in structure that result in a reduced probability of TPeA interaction.

ShBPs. Evidence for the involvement of cytosolic cavity–lining hydrophobic residues in the stabilization of blocking inactivation peptides in K^+ channels comes from the observation that substitution of individual helix residues with amino acids of lower hydrophobicity decreases peptide blocker efficiency (Zhou et al., 2001). Although our data clearly establish that hydrophobic interactions contribute to stabilization of bound blocking peptide, lowering the hydrophobicity of individual residues in TM10 of RyR2 does not destabilize the bound peptide. This could mean that these residues play no role in block or, more likely, that the mechanisms governing *Sh*BP interaction in RyR2 differ from those operating in K^+ channels.

Zhou et al. (2001) demonstrated that residue substitution in cavity-lining K^+ channel helices had broadly similar consequences for the blocking efficiency of both inactivation peptides and TBA, indicating that these different blocking molecules shared sites of interaction and a common mechanism of block. As outlined in the preceding section (TAA cations), our investigations of TAA block of RyR2 indicate that the detailed mechanisms of TAA block in RyR2 and K^+ channels differ. Whereas TAA stabilization in K^+ channels involves hydrophobic interaction with specific residues, large TAAs are most likely stabilized in RyR2 by more diffuse hydrophobic interactions with several residues of one or more wall-lining helix. In such a mechanism, reducing the hydrophobicity of individual helix residues does not produce a dramatic destabilization as the majority of the contributing residues remain. The consequences of lowering the hydrophobicity of individual residues of a helix might be expected to be even less dramatic for the stabilization of bound *Sh*BP than TAA cations, reflecting a broader distribution of hydrophobicity along the length of the peptide when compared with the smaller cations and the potential involvement of more helix residues in holding the bound peptide. Our results are consistent with this proposal.

Correlations between experimental data and the location of residues in the analogy model of the RyR2 PFR

Although we observe some variation in the consequences of alanine substitution of individual TM10 residues, it would be unwise to attempt to correlate these changes with specific locations or to attempt to define binding sites within the PFR model. At best, the model provides us with a prediction of the arrangement of likely components of the RyR2 PFR. Experiments such as those reported here are undertaken to test these predictions. An inspection of the arrangement of the hydrophobic residues examined in this study demonstrates that they appear to be distributed around the TM10 helix in the model with some facing into, and some away from, the cytosolic vestibule (Fig. 4). The template used in the generation of this model is KcsA, and as a result, the model most likely represents a closed conformation of the RyR2 pore. To date we have no information on the mechanisms involved in RyR2 channel opening or the structure of the open pore; however, it is probable that in the open conformation the orientation and location of TM10 residues will differ from that shown in Fig. 4. More significantly, our data indicate that stabilization of TAAs and *Sh*BPs in the RyR2 PRF likely depends on diffuse interactions involving several hydrophobic residues, rather than with specific hydrophobic residues as is the case in K^+ channels.

Conclusion

The data presented in this study reveal important new information on both the mechanisms and structural components of the RyR2 PFR involved in block by large TAAs and *Sh*BPs. Our experiments also highlight important differences in the mechanisms and structures underpinning large TAA and *Sh*BP block in RyR2 and K^+ channels. The data add support to the proposal that although the PFRs of these channels share analogous structural components, differences in the dimensions

and characteristics of domains and residues within the two structures determine the different ion-handling properties of the two species of channel.

We thank Professor William Welch (University of Nevada, Reno, Reno, NV) for measurements of the radius of gyration of the TAA cations used in this study and Matthew Davies, Dr. Ian Brewis, and Professor John Wilson (all Cardiff University School of Medicine, Cardiff, Wales, UK) for technical assistance.

We are grateful to the British Heart Foundation for financial support.

Christopher Miller served as editor.

Submitted: 22 June 2012
Accepted: 6 August 2012

REFERENCES

Armstrong, C.M. 1971. Interaction of tetraethylammonium ion derivatives with the potassium channels of giant axons. *J. Gen. Physiol.* 58:413–437. http://dx.doi.org/10.1085/jgp.58.4.413

Bers, D.M. 2002. Cardiac excitation-contraction coupling. *Nature.* 415:198–205. http://dx.doi.org/10.1038/415198a

Chen, S.R.W., P. Li, M.C. Zhao, X.L. Li, and L. Zhang. 2002. Role of the proposed pore-forming segment of the Ca^{2+} release channel (ryanodine receptor) in ryanodine interaction. *Biophys. J.* 82: 2436–2447. http://dx.doi.org/10.1016/S0006-3495(02)75587-2

Choi, K.L., C. Mossman, J. Aubé, and G. Yellen. 1993. The internal quaternary ammonium receptor site of *Shaker* potassium channels. *Neuron.* 10:533–541. http://dx.doi.org/10.1016/0896-6273(93)90340-W

Cordero-Morales, J.F., L.G. Cuello, Y. Zhao, V. Jogini, D.M. Cortes, B. Roux, and E. Perozo. 2006. Molecular determinants of gating at the potassium-channel selectivity filter. *Nat. Struct. Mol. Biol.* 13:311–318. http://dx.doi.org/10.1038/nsmb1069

Doyle, D.A., J. Morais Cabral, R.A. Pfuetzner, A.L. Kuo, J.M. Gulbis, S.L. Cohen, B.T. Chait, and R. MacKinnon. 1998. The structure of the potassium channel: molecular basis of K^+ conduction and selectivity. *Science.* 280:69–77. http://dx.doi.org/10.1126/science.280.5360.69

Faraldo-Gómez, J.D., E. Kutluay, V. Jogini, Y. Zhao, L. Heginbotham, and B. Roux. 2007. Mechanism of intracellular block of the KcsA K^+ channel by tetrabutylammonium: insights from X-ray crystallography, electrophysiology and replica-exchange molecular dynamics simulations. *J. Mol. Biol.* 365:649–662. http://dx.doi.org/10.1016/j.jmb.2006.09.069

Fernandez-Ballester, G., F. Gavilanes, J.P. Albar, M. Criado, J.A. Ferragut, and J.M. Gonzalez-Ros. 1995. Adoption of β structure by the inactivating "ball" peptide of the *Shaker* B potassium channel. *Biophys. J.* 68:858–865. http://dx.doi.org/10.1016/S0006-3495(95)80262-6

Foster, C.D., S. Chung, W.N. Zagotta, R.W. Aldrich, and I.B. Levitan. 1992. A peptide derived from the *Shaker* B K^+ channel produces short and long blocks of reconstituted Ca^{2+}-dependent K^+ channels. *Neuron.* 9:229–236. http://dx.doi.org/10.1016/0896-6273(92)90162-7

French, R.J., and J.J. Shoukimas. 1981. Blockage of squid axon potassium conductance by internal tetra-N-alkylammonium ions of various sizes. *Biophys. J.* 34:271–291. http://dx.doi.org/10.1016/S0006-3495(81)84849-7

Gasteiger, E., C. Hoogland, A. Gattiker, S. Duvaud, M.R. Wilkins, R.D. Appel, and A. Bairoch. 2005. Protein identification and analysis tools on the ExPASy server. *In* The Proteomics Protocols Handbook. J.M. Walker, editor. Humana Press, Totowa, NJ. 571–607.

George, C.H., and F.A. Lai. 2007. Developing new anti-arrhythmics: clues from the molecular basis of cardiac ryanodine receptor (RyR2) Ca^{2+}-release channel dysfunction. *Curr. Pharm. Des.* 13: 3195–3211. http://dx.doi.org/10.2174/138161207782341259

George, C.H., H. Jundi, N.L. Thomas, D.L. Fry, and F.A. Lai. 2007. Ryanodine receptors and ventricular arrhythmias: emerging trends in mutations, mechanisms and therapies. *J. Mol. Cell. Cardiol.* 42:34–50. http://dx.doi.org/10.1016/j.yjmcc.2006.08.115

Hille, B. 2001. Ionic Channels of Excitable Membranes. Third edition. Sinauer Associates, Inc., Sunderland, MA. 814 pp.

Hilliard, F.A., D.S. Steele, D. Laver, Z. Yang, S.J. Le Marchand, N. Chopra, D.W. Piston, S. Huke, and B.C. Knollmann. 2010. Flecainide inhibits arrhythmogenic Ca^{2+} waves by open state block of ryanodine receptor Ca^{2+} release channels and reduction of Ca^{2+} spark mass. *J. Mol. Cell. Cardiol.* 48:293–301. http://dx.doi.org/10.1016/j.yjmcc.2009.10.005

Jiang, Y.X., A. Lee, J. Chen, M. Cadene, B.T. Chait, and R. MacKinnon. 2002. The open pore conformation of potassium channels. *Nature.* 417:523–526. http://dx.doi.org/10.1038/417523a

Kyte, J., and R.F. Doolittle. 1982. A simple method for displaying the hydropathic character of a protein. *J. Mol. Biol.* 157:105–132. http://dx.doi.org/10.1016/0022-2836(82)90515-0

Lenaeus, M.J., M. Vamvouka, P.J. Focia, and A. Gross. 2005. Structural basis of TEA blockade in a model potassium channel. *Nat. Struct. Mol. Biol.* 12:454–459. http://dx.doi.org/10.1038/nsmb929

Lindsay, A.R.G., A. Tinker, and A.J. Williams. 1994. How does ryanodine modify ion handling in the sheep cardiac sarcoplasmic reticulum $Ca^{(2+)}$-release channel? *J. Gen. Physiol.* 104:425–447. http://dx.doi.org/10.1085/jgp.104.3.425

McGarry, S.J., and A.J. Williams. 1994. Activation of the sheep cardiac sarcoplasmic reticulum Ca^{2+}-release channel by analogues of sulmazole. *Br. J. Pharmacol.* 111:1212–1220. http://dx.doi.org/10.1111/j.1476-5381.1994.tb14874.x

Mead, F.C., and A.J. Williams. 2002. Block of the ryanodine receptor channel by neomycin is relieved at high holding potentials. *Biophys. J.* 82:1953–1963. http://dx.doi.org/10.1016/S0006-3495(02)75544-6

Mead, F.C., D. Sullivan, and A.J. Williams. 1998. Evidence for negative charge in the conduction pathway of the cardiac ryanodine receptor channel provided by the interaction of K^+ channel N-type inactivation peptides. *J. Membr. Biol.* 163:225–234. http://dx.doi.org/10.1007/s002329900386

Mead-Savery, F.C., R. Wang, B. Tanna-Topan, S.R.W. Chen, W. Welch, and A.J. Williams. 2009. Changes in negative charge at the luminal mouth of the pore alter ion handling and gating in the cardiac ryanodine-receptor. *Biophys. J.* 96:1374–1387. http://dx.doi.org/10.1016/j.bpj.2008.10.054

Miller, C. 1982. Open-state substructure of single chloride channels from Torpedo electroplax. *Philos. Trans. R. Soc. Lond. B Biol. Sci.* 299:401–411. http://dx.doi.org/10.1098/rstb.1982.0140

Molina, M.L., F.N. Barrera, J.A. Encinar, M.L. Renart, A.M. Fernández, J.A. Poveda, J. Santoro, M. Bruix, F. Gavilanes, G. Fernández-Ballester, et al. 2008. N-type inactivation of the potassium channel KcsA by the Shaker B "ball" peptide: mapping the inactivating peptide-binding epitope. *J. Biol. Chem.* 283: 18076–18085. http://dx.doi.org/10.1074/jbc.M710132200

Murrell-Lagnado, R.D., and R.W. Aldrich. 1993. Interactions of amino terminal domains of *Shaker* K channels with a pore blocking site studied with synthetic peptides. *J. Gen. Physiol.* 102: 949–975. http://dx.doi.org/10.1085/jgp.102.6.949

Neira, J.L. 2009. The positively charged C-terminal region of the inactivating Shaker B peptide binds to the potassium channel KcsA.

Protein Eng. Des. Sel. 22:341–347. http://dx.doi.org/10.1093/protein/gzp010

Rogers, K.S., and E.S. Higgins. 1973. Lipophilic interactions of organic cations with mitochondrial inner membranes during respiratory control. *J. Biol. Chem.* 248:7142–7148.

Shealy, R.T., A.D. Murphy, R. Ramarathnam, E. Jakobsson, and S. Subramaniam. 2003. Sequence-function analysis of the K^+-selective family of ion channels using a comprehensive alignment and the KcsA channel structure. *Biophys. J.* 84:2929–2942. http://dx.doi.org/10.1016/S0006-3495(03)70020-4

Sitsapesan, R., and A.J. Williams. 1994. Gating of the native and purified cardiac SR $Ca^{(2+)}$-release channel with monovalent cations as permeant species. *Biophys. J.* 67:1484–1494. http://dx.doi.org/10.1016/S0006-3495(94)80622-8

Tanna, B., W. Welch, L. Ruest, J.L. Sutko, and A.J. Williams. 1998. Interactions of a reversible ryanoid (21-amino-9α-hydroxyryanodine) with single sheep cardiac ryanodine receptor channels. *J. Gen. Physiol.* 112:55–69. http://dx.doi.org/10.1085/jgp.112.1.55

Tanna, B., W. Welch, L. Ruest, J.L. Sutko, and A.J. Williams. 2003. An anionic ryanoid, 10-O-succinoylryanodol, provides insights into the mechanisms governing the interaction of ryanoids and the subsequent altered function of ryanodine-receptor channels. *J. Gen. Physiol.* 121:551–561. http://dx.doi.org/10.1085/jgp.200208753

Toro, L., M. Ottolia, E. Stefani, and R. Latorre. 1994. Structural determinants in the interaction of *Shaker* inactivating peptide and a Ca^{2+}-activated K^+ channel. *Biochemistry.* 33:7220–7228. http://dx.doi.org/10.1021/bi00189a026

Valenzuela, C., E. Delpón, M.M. Tamkun, J. Tamargo, and D.J. Snyders. 1995. Stereoselective block of a human cardiac potassium channel (Kv1.5) by bupivacaine enantiomers. *Biophys. J.* 69:418–427. http://dx.doi.org/10.1016/S0006-3495(95)79914-3

Wang, R., L. Zhang, J. Bolstad, N. Diao, C. Brown, L. Ruest, W. Welch, A.J. Williams, and S.R.W. Chen. 2003. Residue Gln4863 within a predicted transmembrane sequence of the Ca^{2+} release channel (ryanodine receptor) is critical for ryanodine interaction. *J. Biol. Chem.* 278:51557–51565. http://dx.doi.org/10.1074/jbc.M306788200

Welch, W., S. Rheault, D.J. West, and A.J. Williams. 2004. A model of the putative pore region of the cardiac ryanodine receptor channel. *Biophys. J.* 87:2335–2351. http://dx.doi.org/10.1529/biophysj.104.044180

West, D.J., and A.J. Williams. 2007. Pharmacological regulators of intracellular calcium release channels. *Curr. Pharm. Des.* 13:2428–2442. http://dx.doi.org/10.2174/138161207781368620

Williams, A.J. 1995. The measurement of the function of ion channels reconstituted into artificial membranes. *In* Ion channels: A practical approach. R.H. Ashley, editor. IRL Press, Oxford. 43–67.

Williams, A.J., D.J. West, and R. Sitsapesan. 2001. Light at the end of the $Ca^{(2+)}$-release channel tunnel: structures and mechanisms involved in ion translocation in ryanodine receptor channels. *Q. Rev. Biophys.* 34:61–104. http://dx.doi.org/10.1017/S0033583501003675

Yohannan, S., Y. Hu, and Y. Zhou. 2007. Crystallographic study of the tetrabutylammonium block to the KcsA K^+ channel. *J. Mol. Biol.* 366:806–814. http://dx.doi.org/10.1016/j.jmb.2006.11.081

Zagotta, W.N., T. Hoshi, and R.W. Aldrich. 1990. Restoration of inactivation in mutants of Shaker potassium channels by a peptide derived from ShB. *Science.* 250:568–571. http://dx.doi.org/10.1126/science.2122520

Zhou, M., J.H. Morais-Cabral, S. Mann, and R. MacKinnon. 2001. Potassium channel receptor site for the inactivation gate and quaternary amine inhibitors. *Nature.* 411:657–661. http://dx.doi.org/10.1038/35079500

Zorzato, F., J. Fujii, K. Otsu, M. Phillips, N.M. Green, F.A. Lai, G. Meissner, and D.H. MacLennan. 1990. Molecular cloning of cDNA encoding human and rabbit forms of the Ca^{2+} release channel (ryanodine receptor) of skeletal muscle sarcoplasmic reticulum. *J. Biol. Chem.* 265:2244–2256.